ChemComm

COMMUNICATION

View Article Online
View Journal | View Issue

Cite this: *Chem. Commun.*, 2025, **61**, 2540

Received 25th September 2024,
Accepted 3rd January 2025

DOI: 10.1039/d4cc04991h

rsc.li/chemcomm

Biochar boost: revolutionizing functionalization of a difficult material†

Sara M. K. Cheema, *[a] Celine M. Schneider,[a] Jean-François Morin, [b] Pascale Chevallier,[b] T. Jane Stockmann, [a] Francesca M. Kerton [a] and Stephanie L. MacQuarrie[ac]

The challenge with synthetically modified biochars is that they are notoriously difficult to characterize, and a new characterization approach that circumvents the challenges posed by overlapping bands in IR spectra is needed. We report multinuclear NMR approaches successful in the easy identification and quantification of covalently-bound functional groups on the biochar surface using $^{31}P\{^{1}H\}$ CPMAS NMR spectroscopy.

Characterizing surface-modified heterogeneous carbon materials such as biochar has been a massive obstacle for researchers; this limits the understanding of these intricate carbon materials and causes challenges in optimizing their application. Biochar has been identified as an essential tool in carbon sequestration by the UN intergovernmental panel on climate change.[1] Biochar has remarkable versatility and unlimited potential for various applications when chemically modified. Various reports suggest that biochar enhancement *via* surface modifications increases its potential for specific renewable material applications. Covalently linking phosphorus groups on biochar is important for soil amendment, water remediation and environmental remediation applications.[2–5] Surface modified biochar demonstrates specific physical properties that allow for optimal use in catalysis, dye removal and heavy metal adsorption.[6–8] For example, Zhong *et al.* synthesized sulfonated biochar *via* diazo grafting methods. This catalytic biochar, which can replace toxic fluoride sulfonic acid, has increased acidity, hydrophobicity, and reusability.[6] Zhong *et al.* confirmed the added sulfonated functional groups using IR, XPS, and TEM spectroscopy with elemental mapping capabilities. Another example of altering biochar's physical properties *via* surface modification is reported by Dong *et al.*, who synthesized a magnetic biochar sulfonic acid catalyst for use in synthesizing spiro-pyrazolo[3,4-*b*]pyridine derivatives from simple materials.[9] Additionally, biochar magnetization simplifies catalyst purification *via* magnetic separation and retains reusability, making it desirable for use in industry.[9] Many groups rely on these characterization methods as well as SEM-EDX and TGA, which are commonly used to confirm the modification of biochar; however, surface analysis methods are only reliable for material with bulk functionalization (> ppm scale). Functional group-specific characterization, such as XPS and IR spectroscopy, confirms functionalization directly on most materials. However, due to biochar's heterogeneity, IR spectroscopy has limitations due to overlapping broad bands from abundant pre-existing functional groups such as C–O, –OH and –C=C– on the surface. Silane condensation reactions have been used to install both simple and versatile functional groups on biochar materials.[5,7,8] Mosaffa *et al.* used 3-chloropropyltrimethoxysilane (CPTMS) *en route* to a melamine-modified biochar that significantly improved dye contamination in wastewater. The evidence for successful functionalization using CPTMS was confirmed *via* IR vibrational bands for Si–O, Si–C and C–Cl bonds.[7] Zhou *et al.* synthesized iminodiacetic acid-functionalized biochar, for cadmium removal from water, *via* 3-aminopropyltripropyltriethoxysilane (APTES) condensation. The interpretation of IR data was challenging due to the pre-existing –COOH bands in the iminodiacetic acid and the biochar surface.[8] Confirming phosphorous modification on biochar surfaces is difficult; it is limited by IR spectroscopy but is possible with XPS spectroscopy. Zhou *et al.* synthesized a phytic acid modified biochar *via* ball milling with phytic acid and noted a 1.6% increase in phosphorous functionalization through analysis *via* XPS.[10] However, this study provided only partial details on the functional group type that was achieved *via* functionalization.[10] Thus, other methods are needed and a thorough solid-state NMR spectroscopy study can yield both qualitative and quantitative results regarding phosphorus-functionalized biochar. While XPS spectroscopy is a straightforward method for surface characterization to confirm added functional groups, this technique is costly and has limited sensitivity on materials with low degrees of functionalization. Additionally, many chemists cannot access an

[a] *Department of Chemistry, Memorial University of Newfoundland, St. John's Newfoundland and Labrador, A1B 3X7, Canada. E-mail: fkerton@mun.ca*
[b] *Département de Chimie Université Laval, Québec, Québec City, G1V 0A6, Canada*
[c] *Department of Chemistry, Cape Breton University, Sydney, Nova Scotia B1P 6L2, Canada. E-mail: Stephanie_MacQuarrie@cbu.ca*

† Electronic supplementary information (ESI) available. See DOI: https://doi.org/10.1039/d4cc04991h

instrument or the expertise to analyze the data obtained. It is very difficult to validate covalent functionalization of biochar, and we propose multinuclear solid-state NMR spectroscopy as a more straightforward method to provide both qualitative and quantitative data on functionalized biochars.

This work describes the phosphorus functionalization of biochar *via* silane condensation reactions and its characterization through a novel quantification method using an isotopically abundant NMR active nucleus, in this case ^{31}P, using cross-polarization magic angle spinning (CPMAS) solid-state NMR spectroscopy. To increase the surface sites available on biochar for silane condensation reactions to occur more favourably, a modified Hummers' oxidation method was used to generate oxidized biochar.[11,12] Exfoliation by sonication is a crucial step for siloxane condensation functionalization on biochar's surface. This is because biochar naturally aggregates and sonication disrupts the van der Waals interactions, causing an increase in accessible sites for surface functionalization. The oxidized biochar underwent exfoliation to disrupt aggregates based on previous studies that identified oxidized biochar as an excellent candidate for liquid phase exfoliation (LPE).[13] LPE was used on oxidized biochar to increase its surface area and allow a higher degree of silane condensation reactions. Exfoliated oxidized biochar was obtained through use of a hydrogen-bond-accepting solvents such as EtOAc, which could interact favourably during LPE with surface –OH and –COOH functional groups.[13]

On exfoliated and non-exfoliated oxidized biochar, the indirect grafting method, Fig. 1 (top route), involved condensing 3-chloropropyltrimethoxysilane (CPTMS) followed by a quaternization reaction with trioctylphosphine ($P(Oc)_3$). The direct grafting method on exfoliated oxidized biochar's surface, Fig. 1 (bottom route), was completed using 3-(trioctylphosphonium chloride)propyl trimethoxysilane (TOPPTMS Cl^-). The TOPPTMS Cl^- reagent used in the direct method was characterized using ^{31}P solution-state NMR and IR spectroscopy located in ESI.† Yields for all routes were compared to determine the optimal route for synthetic purposes (Tables S1 and S2, ESI†).

Using $^{31}P\{^1H\}$ CPMAS NMR spectroscopy, we confirmed covalent functionalization of a phosphonium moiety bound to biochar. This provides a more complete characterization of biochar modification compared with traditional IR spectroscopic methods. Additionally, we demonstrated the enhanced hydrophobic properties of phosphonium functionalized biochar using surface contact angle measurements. For the indirect route, formations of the intermediate CPTMS-biochar was confirmed using IR spectroscopy by the addition of bands at 696 cm^{-1} and 733 cm^{-1} (Fig. S3, ESI†), representing the characteristic C–Cl and Si–C stretches, respectively, and agrees with results reported by Mosaffa *et al.*[7] We further confirmed functionalization using $^{13}C\{^1H\}$ CPMAS NMR spectroscopy (Fig. 2A–D). The resonances centred at 127 ppm in all ^{13}C NMR spectra represent aromatic regions in the oxidized biochar, CPTMS-biochar and $(C_8H_{17})_3P^+Cl^-$ biochar. This agrees with literature reporting aromatic sp^2 regions in biochar appearing at 111–140 ppm along with 45 ppm signal represents the alkyl regions of biochars.[14–16] The peak broadness highlights the heterogeneity and large variety of aromatic carbons in biochar. When we used the same NMR parameters (*e.g.*, scan number), the functionalization of CPTMS-biochar *via* grafting of CPTMS presented additional carbon signals in $^{13}C\{^1H\}$ CPMAS NMR spectrum at 53 and 23 ppm. These represent $–CH_2–Cl$ and $–CH_2–sp^3$

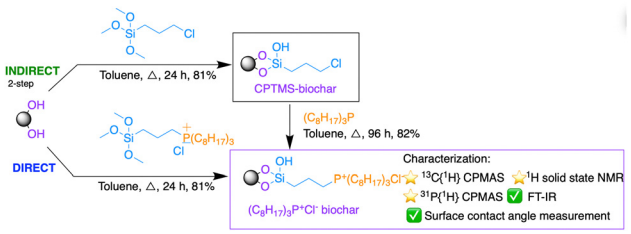

Fig. 1 Biochar modifications and characterization methods used.

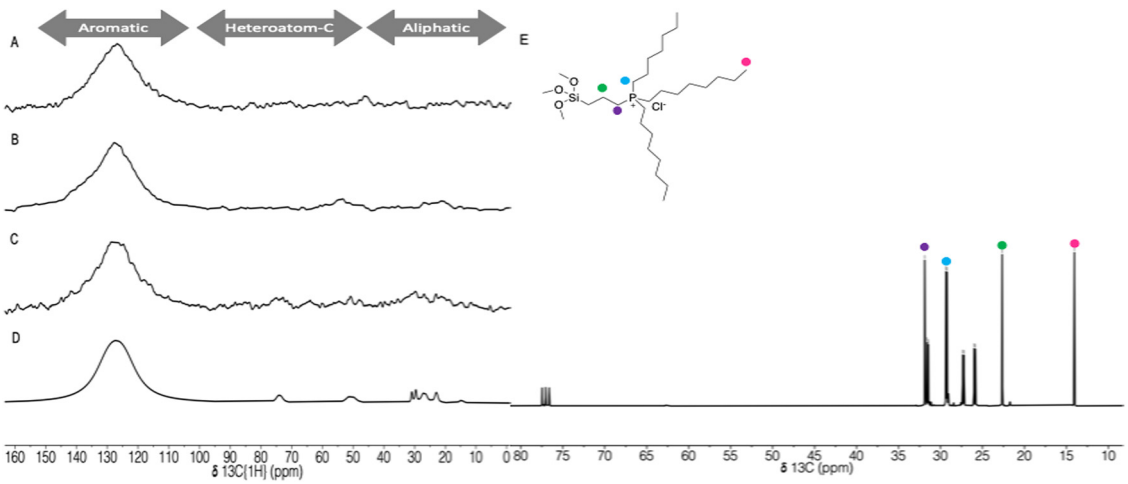

Fig. 2 Left: $^{13}C\{^1H\}$ CPMAS NMR spectra of biochar (A), CPTMS-biochar (B), $(C_8H_{17})_3P^+Cl^-$ biochar (C) and (D) the deconvolution of (C), collected at 600 MHz, vr = 20 kHz, ns = 8k. Right: TOPPTMS Cl^- (E) in solution ^{13}C NMR (75 MHz, $CDCl_3$) δ 31.88, 31.58, 31.44, 29.22, 27.20, 22.65, 14.05. Dots on the spectrum represent atoms in TOPPTMS Cl^-.

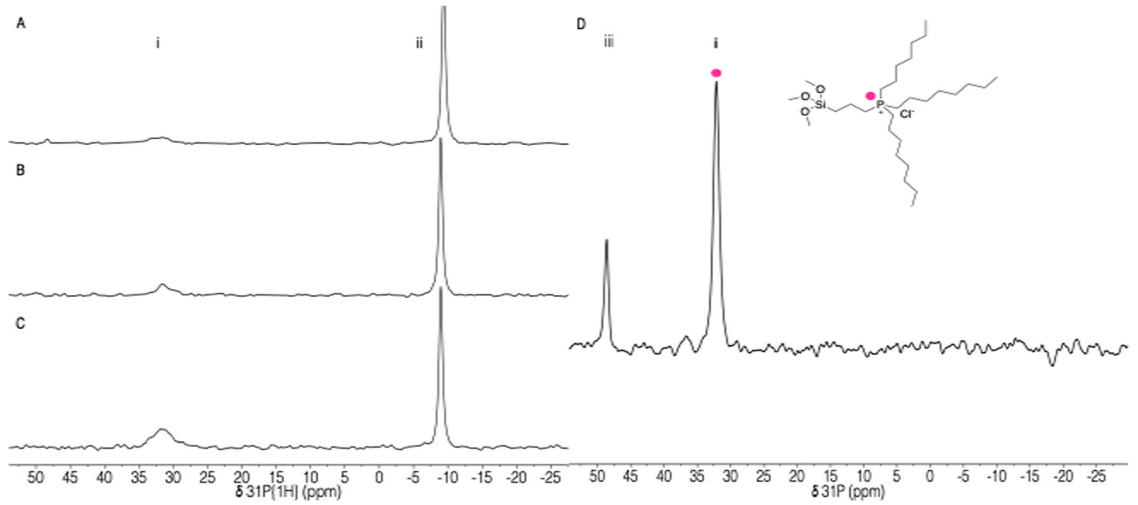

Fig. 3 Left: $^{31}P\{^{1}H\}$ CPMAS NMR spectra of indirect graft non-exfoliated $(C_8H_{17})_3P^+Cl^-$ biochar (A), indirect graft and exfoliated $(C_8H_{17})_3P^+Cl^-$ biochar (B), and direct graft and exfoliated $(C_8H_{17})_3P^+Cl^-$ biochar (C). (i) Quaternary phosphonium, 32 ppm; (ii) P (PPh_3, −9ppm). PPh_3 is used as an internal standard for quantitation. Right: TOPPTMS Cl^- (D) in solution ^{31}P NMR spectra (122 MHz, $CDCl_3$) (iii) trioctylphosphine oxide, 48.61, (i) quaternary phosphonium, 32.13 ppm. Dot on the spectrum represent P atom in TOPPTMS Cl.

carbons, respectively, and Wiench *et al.* reported similar sp^3 carbon peaks when CPTMS was condensed on the surface of MEM-41 (a mesoporous silica).[17] This characterization data provides some evidence for functionalization but it is not a method we can rely on alone to confirm unequivocally or accurately quantify functionalization.

Formation of $(C_8H_{17})_3P^+Cl^-$ biochar *via* nucleophilic addition of $P(Oct)_3$ to CPTMS biochar was suggested by IR data (Fig. S5, ESI†) *via* the presence of pronounced $-CH_2-$ and $-CH_3-$ vibrations. Characterization by $^{13}C\{^{1}H\}$ CPMAS NMR spectroscopy was critical to confirm functionalization, (Fig. 2C and D). The $^{13}C\{^{1}H\}$ CPMAS NMR spectrum of $(C_8H_{17})_3P^+Cl^-$ biochar presents an increase in aliphatic resonances between 14 and 31 ppm. This verifies that octyl groups have been added in line with the ^{13}C NMR spectra of TOPPTMS Cl^- in $CDCl_3$ solution (Fig. 2E). This shows that $^{13}C\{^{1}H\}$ CPMAS NMR can provide valuable qualitative data as proof of biochar modification but to obtain quantitative data, another more abundant NMR active nucleus must be studied.

We decided to use ^{31}P solid-state NMR spectroscopy to study $(C_8H_{17})_3P^+Cl^-$ biochar and quantify the degree of modification, which would be possible due to phosphorus' 100% isotopic abundance compared to ^{13}C (1% abundant) or to ^{29}Si (5% abundant). This allowed both accurate qualitative and quantitative analysis to be achieved alongside the added benefit of shortening the time (scan number) needed to acquire the required data due to its increased sensitivity. Theoretically, this can be applied on any 100% isotopically abundant NMR active nuclei on carbon surfaces. Fig. 3 shows the $^{31}P\{^{1}H\}$ spectrum of TOPPTMS Cl in $CDCl_3$ (Fig. 3D) with a resonance at 32 ppm (xii) assigned to the quaternary phosphonium environment, and an additional resonance from trioctylphosphine oxide contamination at 49 ppm (iii) formed by oxidation of POc_3. Each $^{31}P\{^{1}H\}$ CPMAS NMR spectrum of the grafted phosphonium modified biochars contained a signal at 32 ppm (iv) characteristic of a trialkylphosphonium environment (Table 1).

Table 1 Comparison of % phosphorus levels obtained by $^{31}P\{^{1}H\}$ CPMAS NMR analysis *via* different modification routes (sample calculations are provided in ESI)

Phosphonium modified biochar	Synthesis	Oxidized biochar	%P added (%)
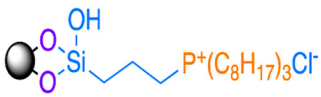	Indirect	Non-Exfoliated	1.3
	Indirect	Exfoliated	11.6
	Direct	Exfoliated	18.0

Functionalization of the biochar was further quantified using an internal standard (triphenylphosphine (PPh_3)) in the $^{31}P\{^{1}H\}$ CPMAS NMR samples to determine the number of phosphonium groups on the biochar surface relative to the standard. This allowed the quantification of the amount of phosphorus on the surface of the modified biochar shown in Table 1. Exfoliation prior to functionalization of the oxidized biochar surface was extremely beneficial and ^{31}P NMR data confirms an increased degree of functionalization with phosphonium ions on the biochar surface. Similar methods have been reported previously to quantify the amount of P in lignin precursors for biofuels.[18]

When comparing the two indirect synthetic pathways, (Table 1 entries 1 and 2), a ten-fold increase in %P was observed when reactions were performed after exfoliation. This is the first report of a significant rise in functionalization through exfoliation. The highest amount of phosphorus added to the surface of the exfoliated oxidized biochar was *via* the direct route, (Table 1 entry 3). The direct synthesis yielded a 6.4% higher %P mass added to the surface compared to the indirect grafting route performed on exfoliated biochar. XPS data was also collected on exfoliated samples for comparison and further confirm successful functionalization of the biochar (Fig. S17 and S18, ESI†).

We further demonstrated the significant change of the material by the drastic change in surface contact angle that demonstrated clear hydrophobicity differences on exfoliated $(C_8H_{17})_3P^+Cl^-$ modified-biochar compared with exfoliated oxidized biochar's hydrophilic character using an experimental setup[19] consisting of a pressed pellet of biochar to measure the angle of the water droplet on the surface (Fig. S14, ESI†).

All oxidized biochar samples had 0° measurements under the same conditions, as the water droplet evenly dispersed across the surface, demonstrating the hydrophilicity of the oxidized material. The surface contact angle of exfoliated $(C_8H_{17})_3P^+Cl^-$ biochar ranged from 114° to 119° (116 ± 2.2°) across three samples, (Table 2), showing that the presence of C8 alkyl chains increased the overall surface hydrophobicity of the char. The slight variance in angle can be attributed to changes in relative humidity.

Table 2 Summary of surface contact angle measurements for modified biochar across 3 samples prepared identically

Exfoliated phosphonium modified biochar	θ (°)	Relative Humidity (%)	
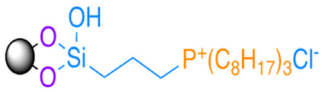	114	39.2	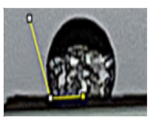
	115	39.4	
	119	39.8	

In this work, direct and indirect routes to produce the first-ever phosphonium-functionalized biochars were explored. We successfully addressed the challenge of providing a more concise way to characterize and quantify modifications of biochar by employing $^{31}P\{^1H\}$ CPMAS NMR spectroscopy. This quantitative method establishes that exfoliation of oxidized biochar before reactions led to increased functionalization. Employing similar solid-state NMR spectroscopic methods for quantitative analysis of modified biochars will allow scientists to more easily correlate physical and chemical properties of the materials, and diversify their use in high value sectors such as energy storage and catalysis.

NSERC of Canada, Memorial University of Newfoundland and Labrador, Cape Breton University and CFI are thanked for operating and infrastructure grants.

Data availability

The data supporting this article have been included as part of the ESI.†

Conflicts of interest

The authors have no conflicts of interest.

References

1 IPCC Intergovernmental Panel on Climate Change. **https://www.ipcc.ch/** (accessed 2023-10-22).
2 IPCC Intergovernmental Panel on Climate Change. **https://www.ipcc.ch/** (accessed 2023-10-22).
3 C. W. W. Ng, *et al.*, *Sci. Rep.*, 2022, **12**(1), 7268.
4 R. Li, *et al.*, *Sci. Total Environ.*, 2024, **917**, 170198.
5 H. Zhang, *et al.*, *J. Hazard. Mater.*, 2020, **390**, 121349.
6 P. Lyu, *et al.*, *Chemosphere*, 2021, **276**, 130116.
7 Y. Zhong, *et al.*, *ACS Sustainable Chem. Eng.*, 2020, **8**(21), 7785.
8 E. Mosaffa, *et al.*, *J. Polym. Environ.*, 2022, **31**, 2486–2503.
9 X. Zhou, *et al.*, *Fuel*, 2018, **233**, 469–479.
10 L.-N. Dong, *et al.*, *Res. Chem. Intermed.*, 2022, **48**(3), 1249.
11 Y. Zhou, *et al.*, *J. Mol. Liq.*, 2020, **303**, 112659.
12 J. Chen, *et al.*, *Carbon*, 2013, **64**, 225–229.
13 W. S. HummersJr and R. E. Offeman, *J. Appl. Chem. Sci.*, 1958, **80**(6), 1339.
14 J. L. Vidal, *ACS Sustainable Chem. Eng.*, 2021, **9**(27), 9114–9125.
15 G. Bonanomi, *et al.*, *PLoS One*, 2015, **10**(1), e0117393.
16 Y. Le Brech, *et al.*, *Anal. Chem.*, 2015, **87**(2), 843–847.
17 G. Bonanomi, F. Ippolito, G. Cesarano, F. Vinale, N. Lombardi and A. Crasto, *et al.*, *Appl. Soil Ecol.*, 2018, **124**, 351–361.
18 J. W. Wiench, *et al.*, *J. Phys. Chem. B*, 2007, **111**(15), 3877–3885.
19 Y. Pu, S. Cao and A. J. Ragauskas, *Energy Environ. Sci.*, 2011, **4**, 3154–3166.
20 M. Zhang, *et al.*, *Processes*, 2022, **10**(2), 301.